Hindawi Publishing Corporation
EURASIP Journal on Advances in Signal Processing
Volume 2010, Article ID 460379, 11 pages
doi:10.1155/2010/460379

Research Article

Iterative Sparse Channel Estimation and Decoding for Underwater MIMO-OFDM

Jie Huang,[1] Jianzhong Huang,[1] Christian R. Berger,[2] Shengli Zhou,[1] and Peter Willett[1]

[1] *Department of Electrical and Computer Engineering, University of Connecticut, 371 Fairfield Way U-2157, Storrs, CT 06269, USA*
[2] *Department of Electrical and Computer Engineering, Carnegie Mellon University, Pittsburgh, PA 15213, USA*

Correspondence should be addressed to Jie Huang, jhuang@engr.uconn.edu

Received 1 November 2009; Revised 20 February 2010; Accepted 8 April 2010

Academic Editor: Tim Davidson

We propose a block-by-block iterative receiver for underwater MIMO-OFDM that couples channel estimation with multiple-input multiple-output (MIMO) detection and low-density parity-check (LDPC) channel decoding. In particular, the channel estimator is based on a compressive sensing technique to exploit the channel sparsity, the MIMO detector consists of a hybrid use of successive interference cancellation and soft minimum mean-square error (MMSE) equalization, and channel coding uses nonbinary LDPC codes. Various feedback strategies from the channel decoder to the channel estimator are studied, including full feedback of hard or soft symbol decisions, as well as their threshold-controlled versions. We study the receiver performance using numerical simulation and experimental data collected from the RACE08 and SPACE08 experiments. We find that iterative receiver processing including sparse channel estimation leads to impressive performance gains. These gains are more pronounced when the number of available pilots to estimate the channel is decreased, for example, when a fixed number of pilots is split between an increasing number of parallel data streams in MIMO transmission. For the various feedback strategies for iterative channel estimation, we observe that soft decision feedback slightly outperforms hard decision feedback.

1. Introduction

Multi-input multi-output (MIMO) techniques have been recently applied in underwater acoustic (UWA) systems to drastically improve the spectral efficiency. Experimental results have been reported in [1–9] for single-carrier systems, and in [6, 10–15] for multicarrier systems, in the form of orthogonal frequency division multiplexing (OFDM).

As we consider MIMO-OFDM in UWA channels, we specify related work: a block-by-block receiver has been developed in [10], where Maximum A Posteriori (MAP) and zero forcing (ZF) detectors are used for MIMO detection following least-squares- (LS-) based channel estimation. Receivers for both spatial multiplexing and differential space time coding have been developed in [11]. Adaptive MIMO detectors have been proposed in [13, 14], where channel estimates based on the previous data block are used for demodulation of the current block after being combined with phase tracking. All the receivers in [10, 11, 13, 14] are noniterative. In [12], an iterative receiver has been presented for MIMO-OFDM that iterates between MIMO detection and channel decoding.

In this paper, we propose an iterative receiver that couples channel estimation, MIMO detection and channel decoding. The differences from [12] are the following.

(1) Channel estimation is included in the iteration loop so that refined channel estimates become available along the iterations.

(2) The LS channel estimator is replaced by a more advanced channel estimator recently tested in [16], that exploits the sparse nature of UWA channels.

When channel estimation is included in the iteration loop, data symbols estimated in the previous round can be utilized as additional training symbols to improve the channel estimation accuracy. We investigate different feedback strategies, including hard decision feedback, soft decision feedback, and their variants that discard unreliable feedback symbols through a thresholding mechanism.

We compare the performance using numerical simulation and experimental data collected from the RACE08 and SPACE08 experiments. Iterative receiver processing leads to impressive performance gains relative to a noniterative receiver.

Note that iterative channel estimation and decoding has been heavily investigated in the literature of wireless radio communications. For example, references [17–19] have considered different hard and soft decision feedback strategies with pilot symbol assisted modulation (PSAM) over time-selective flat-fading channels. References [20, 21] have considered cross-entropy-based hard decision feedback. Specifically to UWA communications, iterative channel estimation and channel decoding has been studied and tested with real data in [22], where only single transmitter OFDM and hard decision feedback are considered. The main contributions of this paper are the followings.

(1) Development of an iterative receiver for underwater MIMO-OFDM, improving upon an existing receiver [12].

(2) Extensive performance testings based on experimental data, showing impressive results for underwater MIMO-OFDM with very high spectral efficiencies.

The rest of this paper is organized as follows. Section 2 introduces the system model. Section 3 presents the details on the iterative receiver. Simulation results are reported in Section 4. Experimental results are reported in Sections 5 and 6 with data collected in RACE08 and SPACE08 experiments, respectively. We conclude in Section 7.

2. System Model

2.1. MIMO-OFDM Transmission. We use zero-padded (ZP) OFDM, as in [12, 23]. Let T denote the OFDM symbol duration and T_g the guard interval. The duration of the overall OFDM block is $T' = T+T_g$ and the subcarrier spacing is $1/T$. The kth subcarrier is at frequency

$$f_k = f_c + \frac{k}{T}, \quad k = -\frac{K}{2}, \ldots, \frac{K}{2} - 1, \tag{1}$$

where f_c is the carrier frequency and K subcarriers are used so that the bandwidth is $B = K/T$.

For an MIMO-OFDM system with N_t transmitters, we use spatial multiplexing to transmit N_t parallel data streams. Specifically, within each OFDM block, N_t independent bit streams are separately encoded with a nonbinary low-density parity-check (LDPC) code [24]. Let $s_\mu[k]$ denote the encoded information symbols, for example, quadratic phase-shift-keying (QPSK) or quadratic amplitude modulation (QAM), to be transmitted on the kth subcarrier by the μth transmitter. The nonoverlapping sets of active subcarriers $\mathcal{S}_A$ and null subcarriers $\mathcal{S}_N$ satisfy $\mathcal{S}_A \cup \mathcal{S}_N = \{-K/2, \ldots, K/2-1\}$; the null subcarriers are used to facilitate Doppler compensation at the receiver [23]. The signal transmitted by the μth transmitter is given by

$$\tilde{x}_\mu(t) = 2\,\mathrm{Re}\left\{\left[\sum_{k\in\mathcal{S}_A} s_\mu[k] e^{j2\pi(k/T)t} q(t)\right] e^{j2\pi f_c t}\right\}, \quad t \in \left[0, T + T_g\right], \tag{2}$$

where $q(t)$ describes the zero-padding operation, that is,

$$q(t) = \begin{cases} 1 & t \in [0, T], \\ 0 & \text{otherwise.} \end{cases} \tag{3}$$

Accounting for all the overheads due to guard interval, channel coding, pilot, and null subcarriers, the overall spectral efficiency in terms of bits per second per Hz (bits/s/Hz) is

$$\alpha = N_t \frac{T}{T+T_g} \frac{|\mathcal{S}_D|}{K} \cdot r_c \log_2 M, \tag{4}$$

where r_c is the code rate, M is the constellation size, and $\mathcal{S}_D \subset \mathcal{S}_A$ is the set of data subcarriers (excluding pilot tones). With bandwidth B, the data rate is $R = \alpha B$ bits per second.

2.2. Receiver Preprocessing. The same receiver preprocessing as in [12] is applied. The received signal can be resampled to compensate a dominant Doppler effect if necessary. After resampling each receiver assumes one common Doppler shift on all transmitted data streams, and uses the energy on the null subcarriers as an objective function to search for the best Doppler shift estimate [12]. Doppler shift compensation is done at each receiver separately.

Let $z_\nu[k]$ denote the output on the kth subchannel at the νth receiver, after the ZP-OFDM demodulation on the received block after Doppler compensation. As in [12], we use the following channel input-output model:

$$z_\nu[k] = \sum_{\mu=1}^{N_t} \tilde{H}_{\nu,\mu}[k] s_\mu[k] + n_\nu[k], \tag{5}$$

where $\tilde{H}_{\nu,\mu}[k]$ is the frequency response between the μth transmitter and the νth receiver at the kth subcarrier, and $n_\nu[k]$ is the additive noise at the demodulator output, which includes both the ambient noise and the residual intercarrier interference (ICI).

3. Iterative Sparse Channel Estimation and Decoding

The proposed iterative receiver processing with N_t transmitters and N_r receivers is shown in Figure 1, where the line represents feedback from the LDPC decoder. We next specify the key modules in the iteration loop: sparse channel estimation, MIMO detection, and channel decoding.

3.1. Sparse Channel Estimation. For each transmitter-receiver pair, we assume a baseband channel with N_p distinct

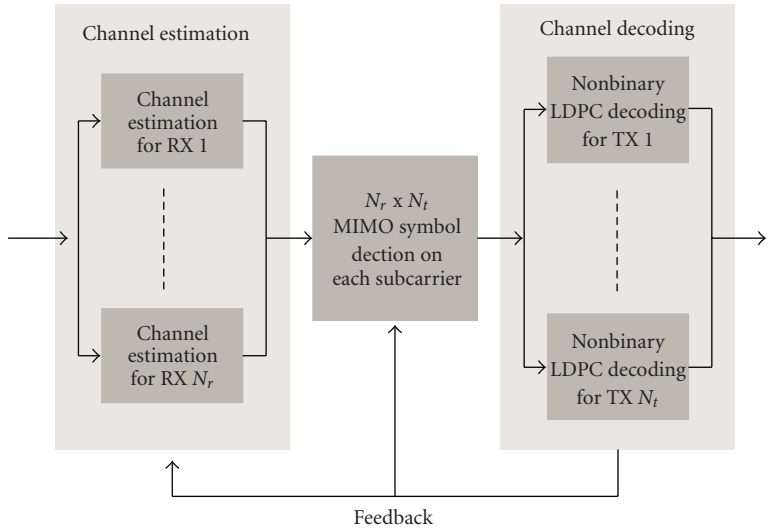

Figure 1: Iterative channel estimation and decoding for MIMO-OFDM.

paths, with each path characterized by a complex amplitude ζ_p and a delay τ_p, (c.f. [16]):

$$h(t) = \sum_{p=1}^{N_p} \zeta_p \delta\left(t - \tau_p\right), \tag{6}$$

such that

$$\widetilde{H}[k] = \sum_{p=1}^{N_p} \zeta_p e^{-j2\pi k(\tau_p/T)}, \tag{7}$$

where we omit the transmitter and receiver index for compact notation.

Define $\widetilde{\mathbf{h}}$ and $\mathbf{w}(\tau_p)$ as column vectors containing $\widetilde{H}[k]$ and $e^{-j2\pi k(\tau_p/T)}$ across subcarriers, respectively. We have

$$\widetilde{\mathbf{h}} = \sum_{p=1}^{N_p} \zeta_p \mathbf{w}\left(\tau_p\right). \tag{8}$$

3.1.1. Overcomplete Delay Dictionary. To formulate the compressed sensing problem, we need to use a large, but finite, dictionary. We discretize τ_p based on the assumption that after synchronization all arriving paths fall into the guard interval, and we choose the time resolution as a fraction, $1/\beta$, of the baseband sampling stepsize T/K, where β is the oversampling factor. In other words, we consider

$$\tau_p \in \left\{0, \frac{T}{\beta K}, \frac{2T}{\beta K}, \ldots, \frac{(N_\tau - 1)T}{\beta K}\right\}, \tag{9}$$

where $N_\tau T/\beta K$ is less than T_g but larger than the channel delay spread. With this we construct a matrix as

$$\mathbf{W} = \left[\mathbf{w}(0) \;\; \mathbf{w}\left(\frac{T}{\beta K}\right) \;\; \cdots \;\; \mathbf{w}\left(\frac{(N_\tau - 1)T}{\beta K}\right)\right], \tag{10}$$

and rewrite (8) as

$$\widetilde{\mathbf{h}} = \mathbf{W}\boldsymbol{\zeta}, \tag{11}$$

where $\boldsymbol{\zeta}$ contains the N_τ possible delays corresponding to the dictionary columns. Since commonly $N_p \ll N_\tau$, $\boldsymbol{\zeta}$ is sparse, that is, it has a limited number of nonzero entries.

Now, we include the transmitter and receiver subscripts, and define $\mathbf{z}_\nu$, $\mathbf{s}_\mu$, and $\mathbf{n}_\nu$ as column vectors whose kth elements are the $z_\nu[k]$, $s_\mu[k]$, and $n_\nu[k]$, respectively. The vector $\mathbf{s}_\mu$ contains known symbols (pilots and symbol estimates from the LDPC decoder). We then have

$$\mathbf{z}_\nu = \sum_{\mu=1}^{N_t} \left[\mathbf{D}_{\mathbf{s}_\mu}\mathbf{W}\right]\boldsymbol{\zeta}_{\nu,\mu} + \mathbf{n}_\nu, \tag{12}$$

where $\mathbf{D}_{\mathbf{s}_\mu}$ is a diagonal matrix with the elements of vector $\mathbf{s}_\mu$ on its main diagonal, and $\boldsymbol{\zeta}_{\nu,\mu}$ contains the N_τ possible delays corresponding to the dictionary columns for the channel from the μth transmitter to the νth receiver.

For a more compact notation, define

$$\begin{aligned} \boldsymbol{\Psi} &= \left[\mathbf{D}_{\mathbf{s}_1}\mathbf{W}, \;\; \mathbf{D}_{\mathbf{s}_2}\mathbf{W}, \;\; \cdots, \;\; \mathbf{D}_{\mathbf{s}_{N_t}}\mathbf{W}\right], \\ \boldsymbol{\zeta}_\nu &= \left[\boldsymbol{\zeta}_{\nu,1}^T, \;\; \boldsymbol{\zeta}_{\nu,2}^T, \;\; \cdots, \;\; \boldsymbol{\zeta}_{\nu,N_t}^T\right]^T, \end{aligned} \tag{13}$$

where $(\cdot)^T$ stands for transpose. We then rewrite (12) as

$$\mathbf{z}_\nu = \boldsymbol{\Psi}\boldsymbol{\zeta}_\nu + \mathbf{n}_\nu, \tag{14}$$

which depends on the pilots and known symbol estimates $s_\mu[k]$ via the matrix $\boldsymbol{\Psi}$.

3.1.2. Basis Pursuit Formulation. Sparse channel estimation can be formulated as a convex optimization problem using what is commonly referred to as l_1-regularization. This

approach is called Basis Pursuit (BP), see for example, [25, 26]. Specifically, BP seeks the solution of

$$\min_{\zeta_\nu} ||\mathbf{z}_\nu - \mathbf{\Psi}\boldsymbol{\zeta}_\nu||^2 + \lambda||\boldsymbol{\zeta}_\nu||_1, \tag{15}$$

where the parameter λ controls the sparsity of the solution $\boldsymbol{\zeta}_\nu$. Note that for a complex vector $\boldsymbol{\zeta}$, its l_1-norm is defined as

$$\|\boldsymbol{\zeta}\|_1 = \sum_{n=1}^{N_t N_r} \sqrt{\mathrm{Re}\,(\zeta_n)^2 + \mathrm{Im}\,(\zeta_n)^2}. \tag{16}$$

An efficient implementation for the complex valued version of BP has been suggested in [26, Section VI.D]. Adopting BP-based sparse channel estimation in multicarrier underwater acoustic communications has been presented in [16], where impressive performance gains over a LS-based channel estimator have been reported. The complexity of BP-based sparse channel estimation, specifically for underwater OFDM systems, is studied in [27].

3.2. MIMO Detection. After estimating the path weights and delays, the frequency response at the data subcarriers can be calculated using (7). At each subcarrier, we stack the received data from N_r receiving-elements [c.f. (5)] as

$$\mathbf{z}[k] = \begin{bmatrix} z_1[k] & \cdots & z_{N_r}[k] \end{bmatrix}^T. \tag{17}$$

Let $\widetilde{\mathbf{H}}[k]$ denote the $N_r \times N_t$ channel matrix whose (ν, μ)-element is $\widetilde{H}_{\nu,\mu}[k]$, and let $\mathbf{s}[k]$ contain N_t transmitted symbols on the kth subcarrier. The matrix-vector channel model for each subcarrier is

$$\mathbf{z}[k] = \widetilde{\mathbf{H}}[k]\mathbf{s}[k] + \mathbf{n}[k], \tag{18}$$

where $\mathbf{n}[k]$ is the additive noise. We assume that the noise on different receivers is uncorrelated and Gaussian distributed.

To demodulate $\mathbf{s}[k]$ from (18), we use the MIMO detector of [12] which consists of a hybrid use of successive interference cancellation and soft minimum mean-square error (MMSE) demodulation; see [12] for details.

3.3. Nonbinary LDPC Decoding. With the outputs from the MMSE equalizer, nonbinary LDPC decoding as in [24] is performed separately for each data stream. The decoder outputs the decoded information symbols and the updated *a posterior*/extrinsic probabilities, which are used in the next iteration of channel estimation and equalization. During the decoding process, if all the parity check conditions of one data stream are satisfied, the decoder declares successful recovery of this data stream. In this case we assume that all symbols of this data stream are known without uncertainty.

To use feedback in channel estimation or MIMO detection, we need estimates of the unknown data and a measure of the uncertainty left in these estimates. Based on the previous round of decoding, the LDPC decoder outputs *a posterior* probabilities for each symbol, as well as probabilities based on extrinsic information only. While the extrinsic information is used in the MIMO symbol detection [12], the *a posterior* probabilities are used to improve channel estimation. Next we investigate different feedback strategies for channel estimation.

3.4. Feedback Strategies. We consider two categories of feedback strategies, namely, hard decision feedback and soft decision feedback. In each category we investigate full feedback and threshold-controlled feedback where the former uses all symbols for feedback and the latter uses only reliable symbols for feedback.

Let $\mathrm{P}_{\mathrm{app}}(s_\mu[k] = \alpha_m)$, $m = 1, \ldots, M$ denote the *a posterior* probability where α_m are the constellation symbols. There are three main feedback strategies in the literature [17–19], varying by the definition of $\widetilde{s}_\mu[k]$—the estimate of $s_\mu[k]$ for channel estimation.

Full Hard Decision Feedback

$$\widetilde{s}_\mu^{(h)}[k] = \alpha_{m^*}, \quad m^* = \arg\max_m \mathrm{P}_{\mathrm{app}}\left(s_\mu[k] = \alpha_m\right). \tag{19}$$

Controlled Hard Decision Feedback

$$\widetilde{s}_\mu^{(th)}[k] = \begin{cases} \widetilde{s}_\mu^{(h)}[k], & H\left(s_\mu[k]\right) < (1 - \Gamma_h)\log_2 M, \\ 0, & \text{otherwise}, \end{cases} \tag{20}$$

where $H(s_\mu[k])$ stands for the entropy calculated from $\mathrm{P}_{\mathrm{app}}(s_\mu[k] = \alpha_m)$ which is the counterpart of the log-likelihood-ratio (LLR) of binary codes and Γ_h is the threshold which lies in $[0, 1]$. In other words, only when the symbol estimate is considered reliable enough, a hard decision is made for feedback.

Full Soft Decision Feedback. One has

$$\widetilde{s}_\mu^{(s)}[k] = \sum_{m=1}^{M} \mathrm{P}_{\mathrm{app}}\left(s_\mu[k] = \alpha_m\right)\alpha_m. \tag{21}$$

In this paper, we further consider a new feedback strategy by applying a threshold on the soft information, where only symbols with the absolute value of their soft estimates larger than a threshold are used.

Controlled Soft Decision Feedback

$$\widetilde{s}_\mu^{(ts)}[k] = \begin{cases} \widetilde{s}_\mu^{(s)}[k], & \displaystyle\sum_{\mu=1}^{N_t} \left|\widetilde{s}_\mu^{(s)}[k]\right| > N_t\Gamma_s|\alpha|_{\max}, \\ 0, & \text{otherwise}, \end{cases} \tag{22}$$

where $|\alpha|_{max}$ is the maximum absolute value of all constellation symbols and Γ_s is the threshold which lies in $[0, 1]$. Here the threshold is applied to the symbols from N_t transmitters jointly. We have also investigated the strategy when a threshold is applied on the symbols from each transmitter individually. The individually controlled feedback strategy has comparable (or worse) performance than the jointly controlled version.

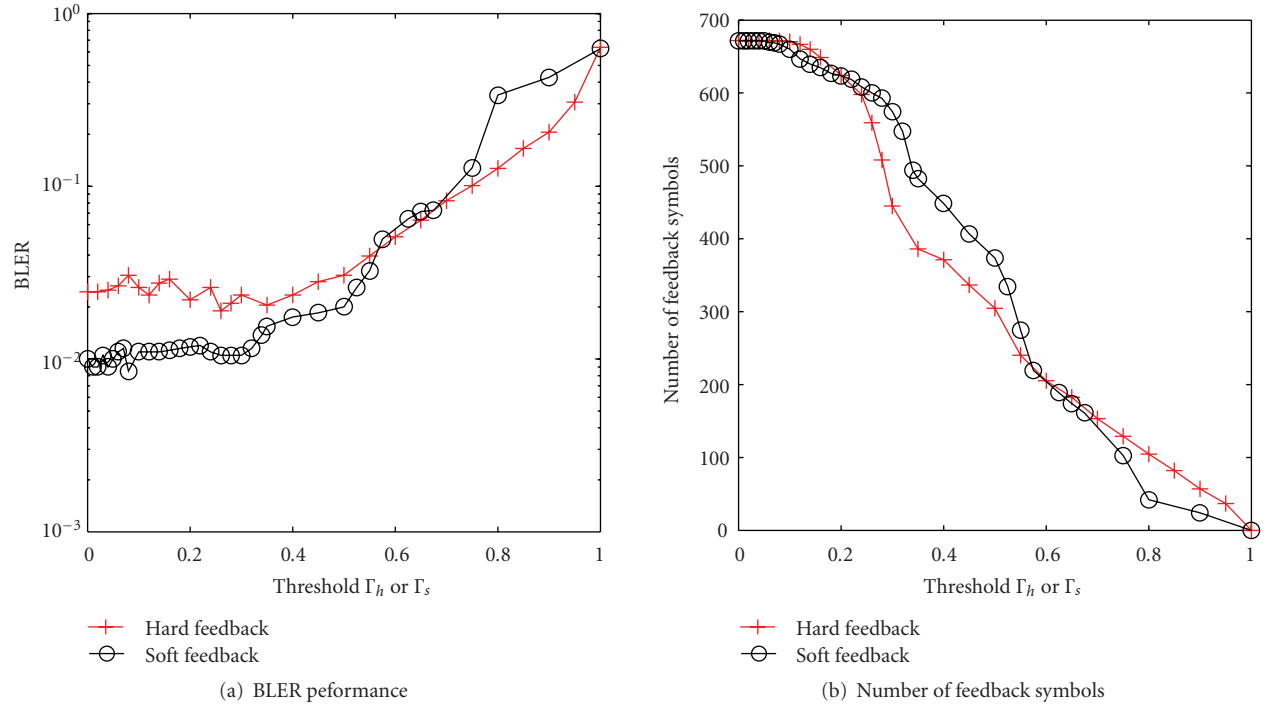

(a) BLER peformance (b) Number of feedback symbols

FIGURE 2: BLER peformance (a) and number of feedback symbols (b) for hard and soft feedback with varying threshold Γ_h or Γ_s; SNR of 2.75 dB.

4. Simulation Results

Consider an OFDM system with the following specifications: carrier frequency $f_c = 13$ kHz, $K = 1024$ subcarriers, symbol duration $T = 104.86$ ms, and guard time $T_g = 24.6$ ms. The bandwidth is then $B = 9.7656$ kHz. It has $|\mathcal{S}_P| = K/4 = 256$ pilot tones and $|\mathcal{S}_N| = 96$ null subcarriers for edge protection and Doppler estimation, leaving $|\mathcal{S}_D| = 672$ data subcarriers. The data within each OFDM symbol is encoded using a rate 1/2 nonbinary LDPC code from [24], and modulated using either QPSK or 16-QAM. These parameters are used in the signal design for the SPACE08 experiment [16, 28].

We consider MIMO systems with $N_t = 2$ or $N_t = 3$ transmitters. With $N_t = 2$, the data rates are 10.4 kb/s and 20.8 kb/s for QPSK and 16-QAM modulations, respectively. With $N_t = 3$, the data rates are 15.6 kb/s and 31.2 kb/s for QPSK and 16-QAM modulations, respectively. The 256 pilots are divided into nonoverlapping sets among all transmitters so that each transmitter has roughly the same number of pilots. The pilot patterns are randomly drawn, rendering irregular positioning [12]. This is usually seen as advantageous in compressed sensing theory, as it can guarantee identifiability of active channel taps with high probability [25].

For the simulation scenario we generate $N_p = 15$ discrete fading paths, where the interarrival times are exponentially distributed with a mean of 1 ms. The amplitude of each path is Rayleigh distributed, with decreasing variance as the delay increases. As each OFDM symbol is encoded separately, we use block-error-rate (BLER) as the figure of merit. In the simulation, each OFDM symbol experiences an independently generated channel. The pilot symbols are drawn from the QPSK constellation whereas the data symbols are drawn from QPSK or 16-QAM constellations. The pilots are scaled to ensure that about one third of the total transmission power is dedicated to channel estimation regardless of the number of transmitters. We simulate the BLER performance at different SNR levels, where SNR is the signal to noise power ratio on the data subcarriers.

In Figure 2 we compare hard decision and soft decision feedback strategies with operating SNR fixed as 2.75 dB for $N_t = 2, N_r = 4$, and 16-QAM modulation. Note that $\Gamma_h = 0$ corresponds to full hard decision feedback and $\Gamma_s = 0$ corresponds to full soft decision feedback. As Γ_h (or Γ_s) increases from 0 to 1, the number of feedback symbols drops all the way from the maximum down to zero. We observe from Figure 2 that a decent number of feedback symbols is necessary to achieve good performance, which means that we need to choose a small value of Γ_h or Γ_s (less than 0.4 in Figure 2). In general, controlled soft decision feedback performs better than hard decision feedback when the threshold Γ_h or Γ_s is small. We also observe that both soft and hard decision feedback strategies are not sensitive to the threshold when it is below a certain value (e.g., 0.4 in the setting of Figure 2).

In Figures 3, 4, 5, and 6 we compare different receivers for two MIMO-OFDM systems where $N_t = 2$ and $N_r = 4$ in Figures 3 and 4, $N_t = 3$ and $N_r = 6$ in Figures 5 and 6. The maximum number of iterations for performing iterative updating between sparse channel estimation, MIMO detection and nonbinary LDPC decoding is 10, where we update

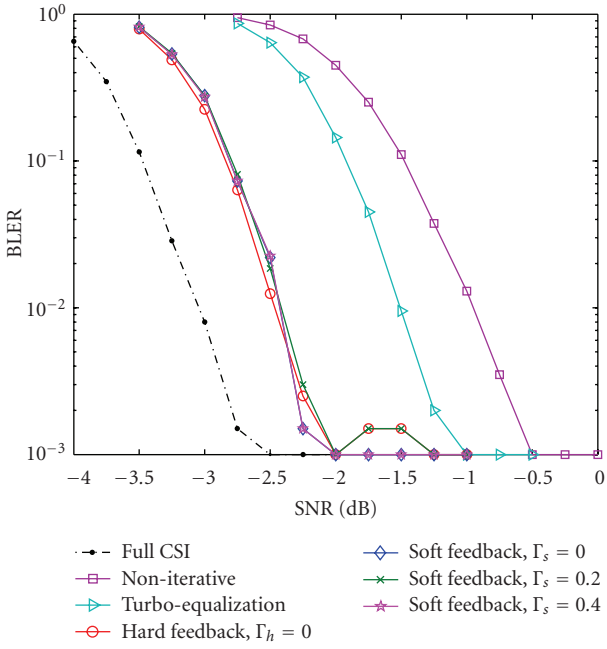

FIGURE 3: Simulation results, $N_t = 2$, $N_r = 4$, QPSK.

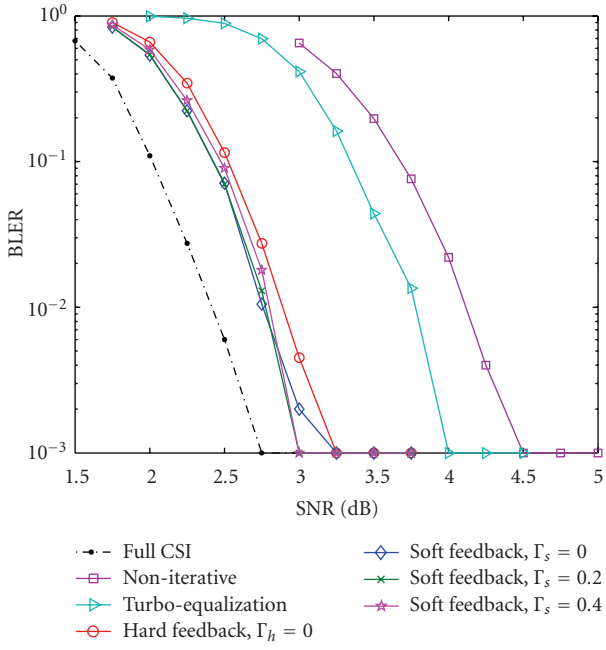

FIGURE 4: Simulation results, $N_t = 2$, $N_r = 4$, 16-QAM.

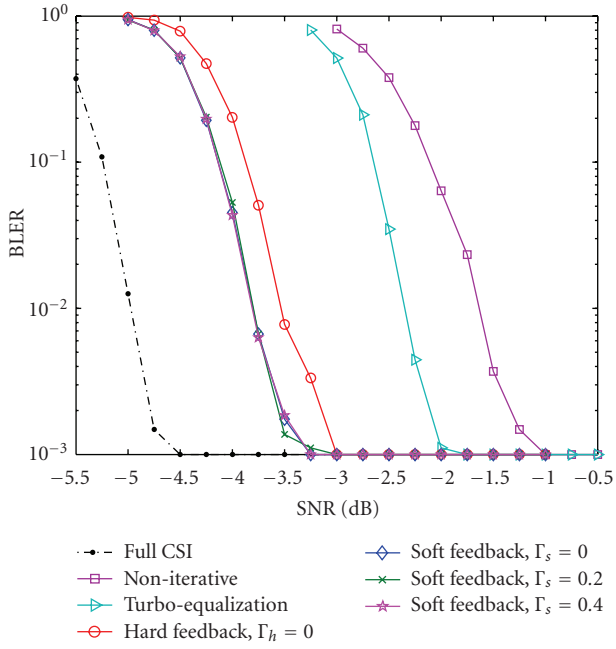

FIGURE 5: Simulation results, $N_t = 3$, $N_r = 6$, QPSK.

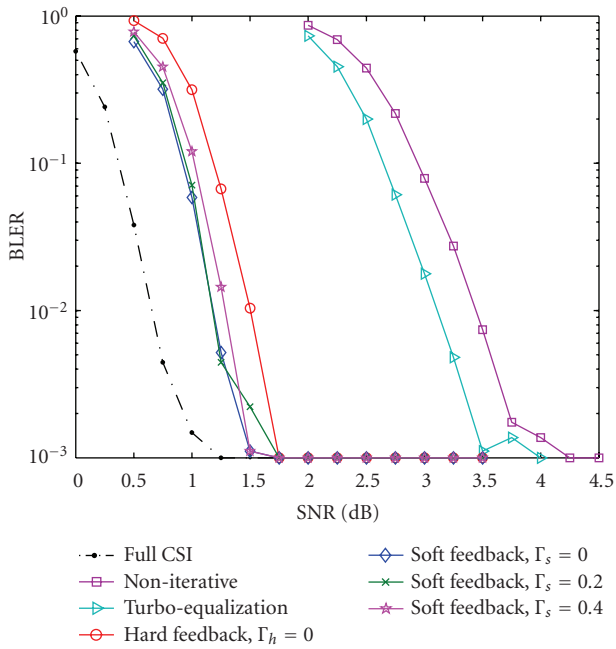

FIGURE 6: Simulation results, $N_t = 3$, $N_r = 6$, 16-QAM.

both the channel estimation and the MIMO detection in each iteration.

The receivers considered are as follows.

(i) "*Non-iterative*" receiver as in [10], but with the LS channel estimator replaced by the BP estimator.

(ii) "*Turbo-equalization*" receiver as in [12], but with the LS channel estimator replaced by the BP estimator.

(iii) The proposed iterative receiver with "*controlled soft decision feedback*" with different thresholds.

(iv) The proposed iterative receiver with "*full hard decision feedback*" (in all subsequent figures, "Non-iterative," "Turbo-equalization," "Soft feedback," and "Hard feedback" are used as legends for different receivers).

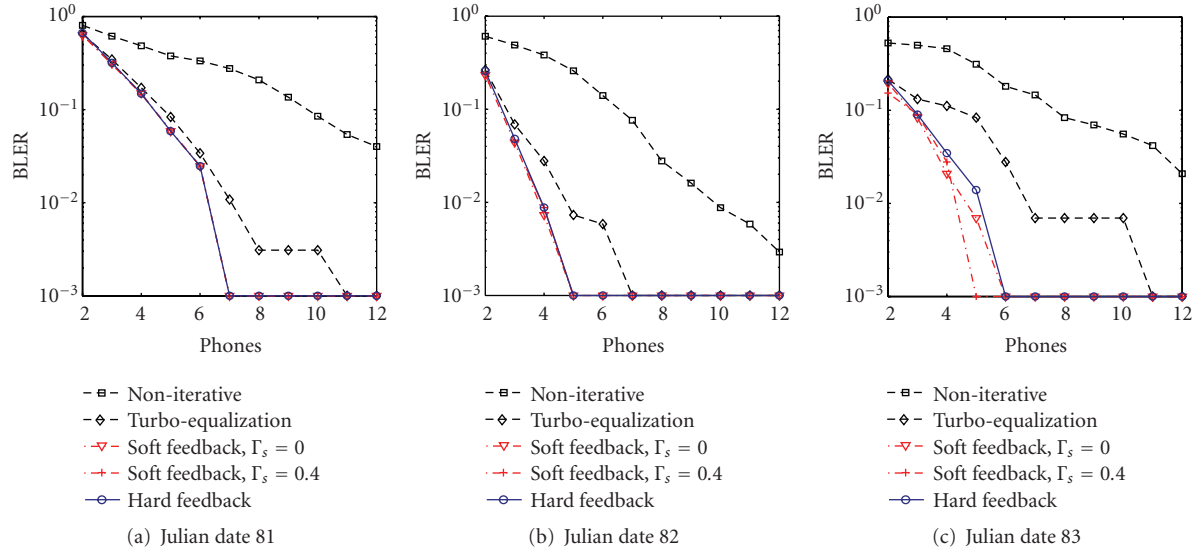

(a) Julian date 81 (b) Julian date 82 (c) Julian date 83

Figure 7: Experimental results from the RACE08 experiment on MIMO-OFDM with $N_t = 2$ and 16-QAM.

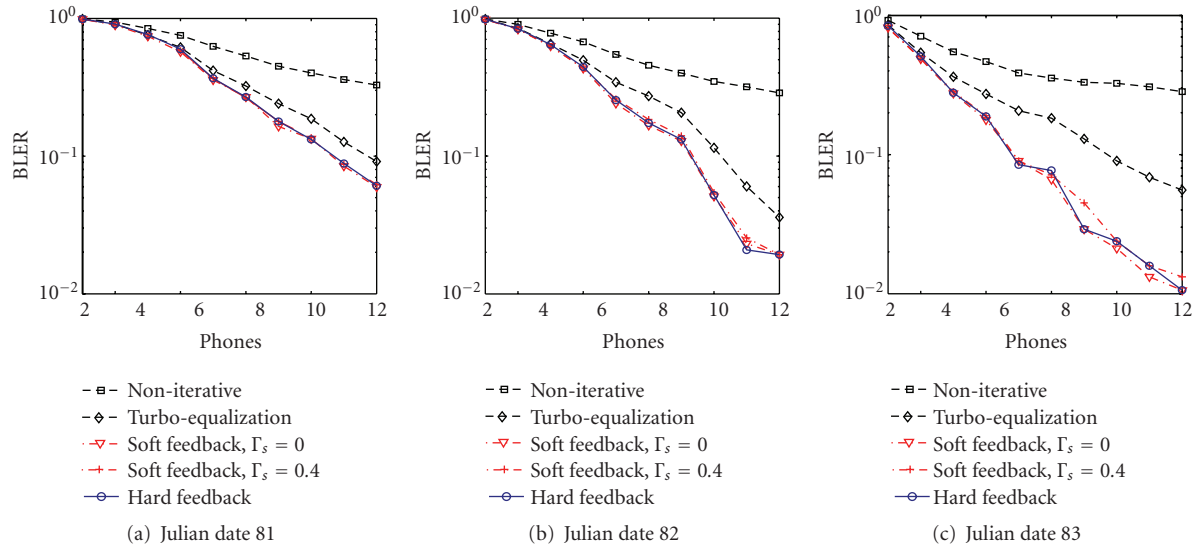

(a) Julian date 81 (b) Julian date 82 (c) Julian date 83

Figure 8: Experimental results from the RACE08 experiment on MIMO-OFDM with $N_t = 3$ and 16-QAM.

Also we include a case with full channel state information (CSI) which still iterates between MIMO detection and LDPC decoding, but has a perfect channel estimate.

Figures 3–6 show that employing a turbo equalization receiver gains about 0.5–1 dB over a noniterative receiver, Including channel estimation in the iteration loop leads to gains of about 1 dB for $N_t = 2$ and 1.5 dB for $N_t = 3$. This seems intuitive, as with an increasing number of transmitters there are less pilots available per data stream, making the "additional pilots" from feedback more valuable. The gap between the proposed receivers and the full CSI case is approximately between 0.5 dB and 1 dB.

In Figure 4 the iterative receiver with full hard decision feedback performs slightly worse than the iterative receivers with soft decision feedback. This gap gets more pronounced when the number of transmitters increases as shown in Figures 5 and 6.

5. Experimental Results: RACE08

The RACE08 experiment was held in the Narragansett Bay, Rhode Island, in March 2008. The water depth in the area is between 9 and 14 meters. The system parameters are the same as in the numerical simulation, except for a different bandwidth of $B = 4.88$ kHz. The corresponding symbol duration and subcarrier spacing are $T = K/B = 209.7$ ms and $1/T = 4.8$ Hz, respectively. More detailed description of the RACE08 experiment can be found in [12, 29].

Table 1: Performance results with high data rates from RACE08; twelve receivers used.

	Spectral efficiency	Data streams	Average BER	Average BLER
3IMO, 64-QAM	5.28 bits/s/Hz	Stream 1	2.8×10^{-1}	9.9×10^{-1}
		Stream 2	6.0×10^{-2}	1.8×10^{-1}
		Stream 3	9.1×10^{-2}	2.7×10^{-1}
4IMO, 16-QAM	4.69 bits/s/Hz	Stream 1	9.4×10^{-2}	4.5×10^{-1}
		Stream 2	2.8×10^{-2}	9.0×10^{-2}
		Stream 3	2.7×10^{-2}	8.3×10^{-2}
		Stream 4	1.6×10^{-2}	5.6×10^{-2}

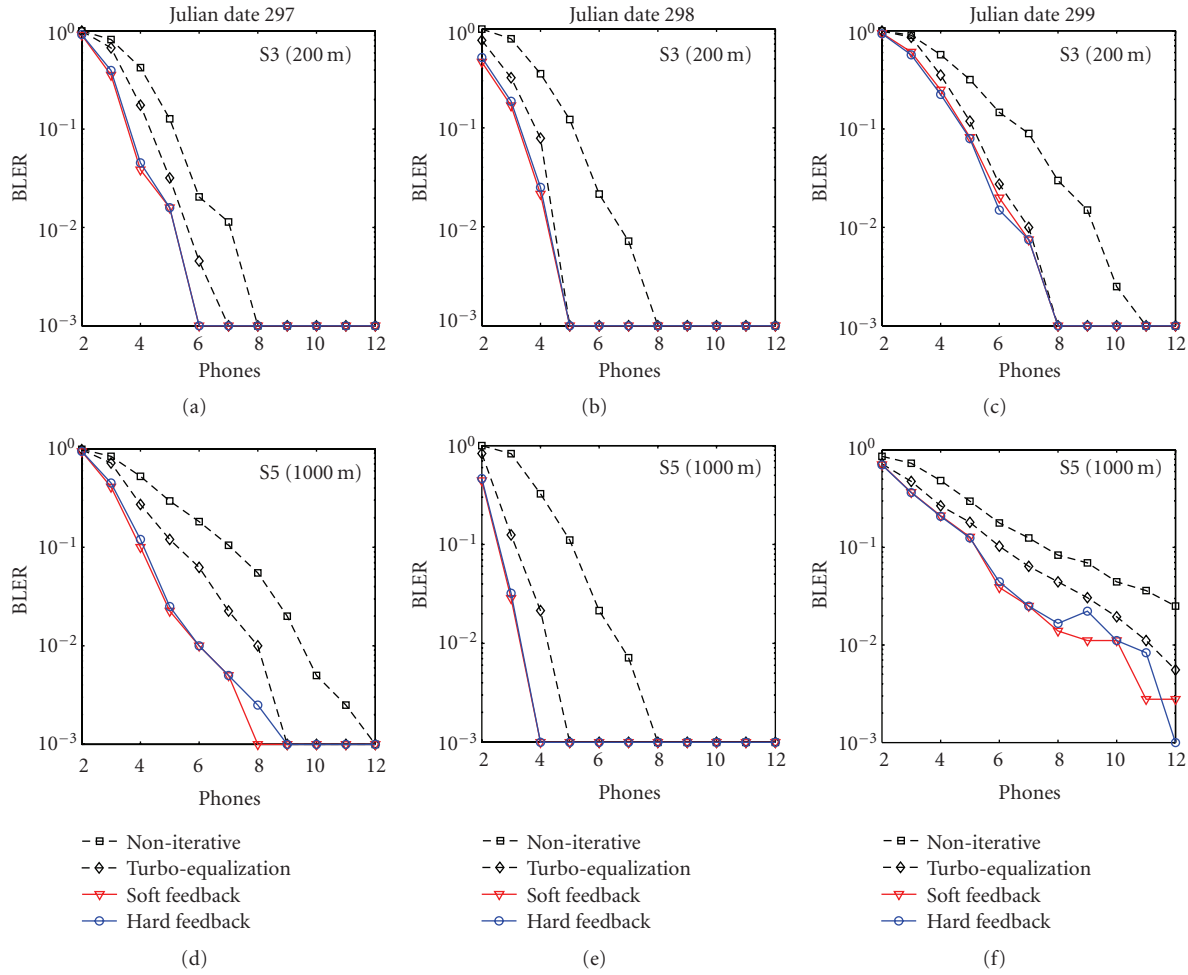

Figure 9: Experimental results from the SPACE08 experiment with $N_t = 2$, QPSK, for S3 (200 m) and S5 (1000 m).

During the experiment, each transmission file was transmitted twice every four hours, leading to 12 transmissions each day. A total of 124 data sets were successfully recorded on each array within 13 days from the Julian date 073 to the Julian date 085. We focus on three days of the experiment, Julian dates 81–83, and receiver S3, which was located 400 m away from the transmitter. We consider 16-QAM and two MIMO setups: one with two transmitters and one with three transmitters. These setups have also been studied in [12] with the turbo-equalization receiver.

The performance results with two transmitters are plotted in Figure 7 and the performance results with three transmitters are plotted in Figure 8. We combine an increasing number of hydrophones to vary effective SNR and to illustrate performance differences. The spacing between consecutive hydrophones is 12 cm. The maximum number of iterations for performing iterative updating between sparse channel estimation, MIMO detection, and nonbinary LDPC decoding is 6. We report the results with the proposed iterative processing with full hard decision feedback and soft

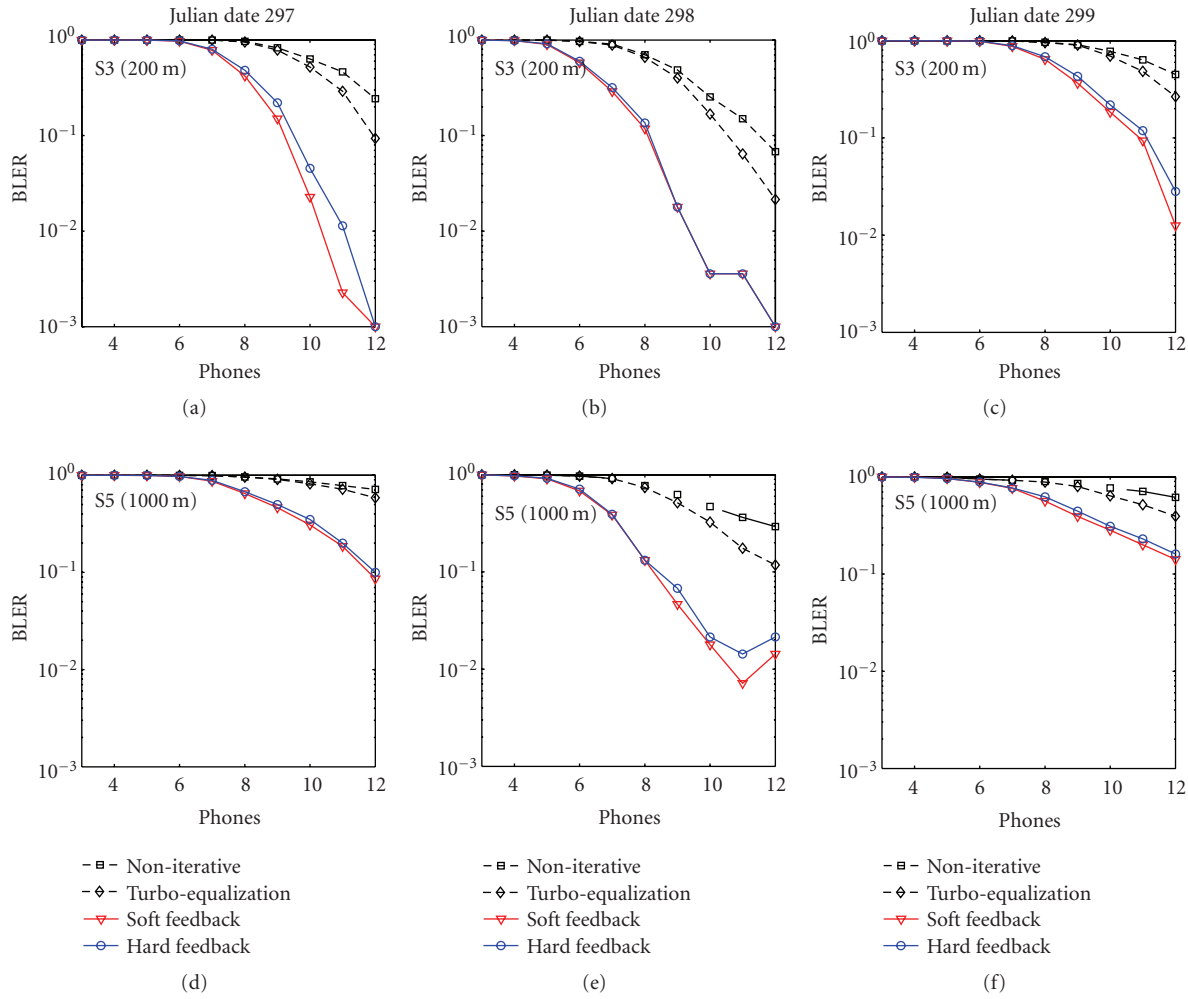

Figure 10: Experimental results from the SPACE08 experiment with $N_t = 3$, QPSK, for S3 (200 m) and S5 (1000 m).

decision feedback with $\Gamma_s = 0$ or $\Gamma_s = 0.4$. Generally an iterative receiver can gain significantly over a noniterative receiver. Besides, all feedback strategies, including full hard decision and soft decision feedback have similar performance on this data set, showing a sizable gain over turbo-equalization.

In Table I, we also include results for two setups not available in [12]: (i) $N_t = 3$, 64-QAM and (ii) $N_t = 4$, 16-QAM, having spectral efficiencies of 5.28 and 4.69 bits/s/Hz, respectively. The results are based on Julian date 83 only, and $N_r = 12$ receive-elements are used. Although data stream one performs poorly due to a transducer issue (see discussion in [12]), the other data streams can be decoded at reasonable levels.

Remark 1. This paper does not include performance results with the LS channel estimator. It has been shown in [16] that the BP-based channel estimator outperforms the LS counterpart considerably. Also, comparing with the turbo equalizer based on the LS channel estimator [12], the turbo equalizer based on the BP channel estimator has considerably better performance. Specifically, in Table III of [12], the turbo-equalization receiver achieves BLER of 1×10^{-2} using twelve phones, for MIMO-OFDM with two transmitters and 16-QAM. Figure 7 in this paper shows that zero BLER is achieved using even less than twelve phones for turbo equalization using the BP channel estimator. Finally, we note that the MIMO-OFDM settings in Table 1 cannot be decoded by the turbo-equalization receiver if coupled with the LS channel estimator as in [12].

6. Experimental Results: SPACE08

The SPACE08 experiment was held off the coast of Martha's Vineyard, MA, from Oct. 14 to Nov. 1, 2008. The water depth is about 15 meters. The spacing between consecutive hydrophones is 12 cm. The detailed description of the SPACE08 experiment can be found in [28, 29].

We focus on receivers S3 and S5 that were located 200 m and We consider recorded data from three consecutive days, Julian date 297 to Julian date 299. For each day, there are twelve recorded files consisting of twenty OFDM symbols each. On the Julian date 298, the five files recorded

during the afternoon were severely distorted and therefore unusable; we focus on the remaining seven files recorded during the morning and evening. Due to the more challenging environment, we only consider the small-size QPSK constellation. The transmission signal model for SPACE08 has the same setup as the simulation setup in Section 4. The data rates for the MIMO system using QPSK modulation are 10.4 kb/s and 15.6 kb/s, when $N_t = 2$ and $N_t = 3$, respectively.

Performance results are plotted in Figure 9 for $N_t = 2$ and in Figure 10 for $N_t = 3$. The maximum number of iterations for performing iterative updating between sparse channel estimation, MIMO detection, and nonbinary LDPC decoding is 6 and we use full soft decision and hard decision feedback. For $N_t = 2$, we observe a sizable gain using updated channel estimates, while all iterative receivers gain significantly over the noniterative receiver. For the $N_t = 3$ setup, the gain of updated channel estimates is more pronounced, matching previous observations in numerical simulation.

Remark 2. For the simulation results in Section 4, we plot the BLER performance as a function of SNR. For the experimental results in Sections 5 and 6, we plot the BLER performance as a function of the number of phones used at the receiver. One common practice to show the performance dependance on SNR based on experimental data is to add recorded ambient noise to the received signals. In this paper, we have not pursued such an approach, which could be explored in the near future.

7. Conclusion

In this paper, we have developed an iterative receiver for underwater MIMO-OFDM that couples sparse channel estimation, MIMO detection, and channel decoding. Various types of feedback information have been considered to improve the sparse channel estimator using the Basis Pursuit algorithm. We tested the proposed receiver extensively using numerical simulation and experimental data for MIMO-OFDM with very large spectral efficiencies. We find that including channel estimation in the iterative loop leads to significant gains in performance. These gains are more pronounced if less pilots are available for channel estimation, for example, when a fixed number of pilots is split between parallel data streams. For the various feedback strategies for iterative channel estimation, we observe that soft decision feedback slightly outperforms hard decision feedback in most cases.

Acknowledgments

This work was supported by the NSF Grant CNS-0721834, the ONR Grants N00014-07-1-0805 (YIP), and N00014-09-1-0704 (PECASE). Part of this work was presented at the MTS/IEEE OCEANS Conference, Biloxi, MS, USA, Oct. 2009.

References

[1] D. B. Kilfoyle, J. C. Preisig, and A. B. Baggeroer, "Spatial modulation experiments in the underwater acoustic channel," *IEEE Journal of Oceanic Engineering*, vol. 30, no. 2, pp. 406–415, 2005.

[2] H. C. Song, P. Roux, W. S. Hodgkiss, W. A. Kuperman, T. Akal, and M. Stevenson, "Multiple-input-multiple-output coherent time reversal communications in a shallow-water acoustic channel," *IEEE Journal of Oceanic Engineering*, vol. 31, no. 1, pp. 170–178, 2006.

[3] S. Roy, T. M. Duman, V. McDonald, and J. G. Proakis, "High-rate communication for underwater acoustic channels using multiple transmitters and space-time coding: receiver structures and experimental results," *IEEE Journal of Oceanic Engineering*, vol. 32, no. 3, pp. 663–688, 2007.

[4] J. Tao, Y. R. Zheng, C. Xiao, T. C. Yang, and W.-B. Yang, "Time-domain receiver design for MIMO underwater acoustic communications," in *Proceedings of the MTS-IEEE Oceans Conference*, Quèbec, Canada, September 2008.

[5] J. Zhang, Y. R. Zheng, and C. Xiao, "Frequency-domain equalization for single carrier MIMO underwater acoustic communications," in *Proceedings of the MTS-IEEE Oceans Conference*, Quèbec, Canada, September 2008.

[6] F. Qu and L. Yang, "Basis expansion model for underwater acoustic channels?" in *Proceedings of the MTS-IEEE Oceans Conference*, Quèbec, Canada, September 2008.

[7] A. Song, M. Badiey, and V. K. McDonald, "Multi-channel combining and equalization for underwater acoustic MIMO channels," in *Proceedings of the MTS-IEEE Oceans Conference*, Quèbec, Canada, September 2008.

[8] J. Ling, T. Yardibi, X. Su, H. He, and J. Li, "Enhanced channel estimation and symbol detection for high speed mutli-input multi-output underwater acoustic communications," *Journal of Acoustical Society of America*, vol. 125, no. 5, pp. 3067–3078, 2009.

[9] J. Zhang, Y. R. Zheng, and C. Xiao, "Frequency-domain turbo equalization for MIMO underwater acoustic communications," in *Proceedings of the MTS-IEEE Oceans Conference*, Bremen, Germany, May 2009.

[10] B. Li, S. Zhou, M. Stojanovic, L. Freitag, J. Huang, and P. Willett, "MIMO-OFDM over an underwater acoustic channel," in *Proceedings of the MTS-IEEE Oceans Conference*, Vancouver, Canada, October 2007.

[11] Y. Emre, V. Kandasamy, T. M. Duman, P. Hursky, and S. Roy, "Multiinput multi-output OFDM for shallow-water UWA communications," in *Proceedings of the IEEE International Conference on Acoustics, Speech, and Signal Processing (ICASSP '08)*, Paris, France, 2008.

[12] B. Li, J. Huang, S. Zhou, et al., "MIMO-OFDM for high rate underwater acoustic communications," *IEEE Journal of Oceanic Engineering*, vol. 34, no. 4, pp. 634–644, 2009.

[13] P. Carrascosa and M. Stojanovic, "Adaptive MIMO detection of OFDM signals in an underwater acoustic channel," in *Proceedings of the MTS-IEEE Oceans Conference*, Quèbec, Canada, September 2008.

[14] M. Stojanovic, "Adaptive channel estimation for underwater acoustic MIMO OFDM systems," in *Proceedings of the IEEE 13th Digital Signal Processing Workshop and 5th IEEE Signal Processing Education Workshop (DSP/SPE '09)*, pp. 132–137, Marco Island, Fla, USA, January 2009.

[15] F. Qu and L. Yang, "Rate and reliability oriented underwater acoustic communication schemes," in *Proceedings of the IEEE*

13th Digital Signal Processing Workshop and 5th IEEE Signal Processing Education Workshop (DSP/SPE '09), pp. 144–149, Marco Island, Fla, USA, January 2009.

[16] C. R. Berger, S. Zhou, J. C. Preisig, and P. Willett, "Sparse channel estimation for multicarrier underwater acoustic communication: from subspace methods to compressed sensing," *IEEE Transactions on Signal Processing*, vol. 58, no. 3, pp. 1708–1721, 2010.

[17] M. C. Valenti and B. D. Woerner, "Iterative channel estimation and decoding of pilot symbol assisted turbo codes over flat-fading channels," *IEEE Journal on Selected Areas in Communications*, vol. 19, no. 9, pp. 1697–1705, 2001.

[18] H. Niu and J. A. Ritcey, "Iterative channel estimation and decoding of pilot symbol assisted LDPC coded QAM over flat fading channels," in *Proceedings of the 37th Asilomar Conference on Signals, Systems and Computers*, vol. 1, pp. 2265–2269, Pacific Grove, Calif, USA, November 2002.

[19] H. Niu, M. Shen, J. A. Ritcey, and H. Liu, "A factor graph approach to iterative channel estimation and LDPC decoding over fading channels," *IEEE Transactions on Wireless Communications*, vol. 4, no. 4, pp. 1345–1350, 2005.

[20] J. Wu, B. R. Vojcic, and Z. Wang, "Turbo decoding complexity reduction by symbol selection and partial iterations," in *Proceedings of the 50th Annual IEEE Global Telecommunications Conference (GLOBECOM '07)*, pp. 3910–3914, Washington, DC, USA, November 2007.

[21] J. Wu, B. R. Vojcic, and Z. Wang, "Cross-entropy based symbol selection and partial iterative decoding for serial concatenated convolutional codes," in *Proceedings of the 42nd Annual Conference on Information Sciences and Systems (CISS '08)*, pp. 1104–1107, Princeton, NJ, USA, March 2008.

[22] T. Kang and R. A. Iltis, "Iterative carrier frequency offset and channel estimation for underwater acoustic OFDM systems," *IEEE Journal on Selected Areas in Communications*, vol. 26, no. 9, pp. 1650–1661, 2008.

[23] B. Li, S. Zhou, M. Stojanovic, F. L. Freitag, and P. Willett, "Multicarrier communication over underwater acoustic channels with nonuniform Doppler shifts," *IEEE Journal of Oceanic Engineering*, vol. 33, no. 2, pp. 198–209, 2008.

[24] J. Huang, S. Zhou, and P. Willett, "Nonbinary LDPC coding for multicarrier underwater acoustic communication," *IEEE Journal on Selected Areas in Communications*, vol. 26, no. 9, pp. 1684–1696, 2008.

[25] D. L. Donoho, "Compressed sensing," *IEEE Transactions on Information Theory*, vol. 52, no. 4, pp. 1289–1306, 2006.

[26] S.-J. Kim, K. Koh, M. Lustig, S. Boyd, and D. Gorinevsky, "An interior-point method for large-scale l_1-regularized least squares," *IEEE Journal on Selected Topics in Signal Processing*, vol. 1, no. 4, pp. 606–617, 2007.

[27] J.-Z. Huang, C. R. Berger, S. Zhou, and J. Huang, "Comparison of basis pursuit algorithms for sparse channel estimation in underwater acoustic OFDM," in *Proceedings of the MTS-IEEE Oceans Conference*, Sydney, Australia, May 24–27, 2010.

[28] C. R. Berger, S. Zhou, W. Chen, and J. Huang, "A simple and effective noise whitening method for underwater acoustic OFDM," in *Proceedings of the MTS-IEEE Oceans Conference*, Biloxi, Miss, USA, October 2009.

[29] L. Freitag and S. Singh, "Performance of micro-modem PSK signalling under variable conditions during the 2008 RACE and SPACE experiments," in *Proceedings of the MTS-IEEE Oceans Conference*, Biloxi, Miss, USA, October 2009.